Development 139, 3332-3342 (2012) doi:10.1242/dev.078063
© 2012. Published by The Company of Biologists Ltd

Convergent repression of Foxp2 3′UTR by miR-9 and miR-132 in embryonic mouse neocortex: implications for radial migration of neurons

Yoanne M. Clovis[1], Wolfgang Enard[2], Federica Marinaro[1], Wieland B. Huttner[3] and Davide De Pietri Tonelli[1,*]

SUMMARY

MicroRNAs (miRNAs) are rapidly emerging as a new layer of regulation of mammalian brain development. However, most of the miRNA target genes remain unidentified. Here, we explore gene expression profiling upon miRNA depletion and in vivo target validation as a strategy to identify novel miRNA targets in embryonic mouse neocortex. By this means, we find that Foxp2, a transcription factor associated with speech and language development and evolution, is a novel miRNA target. In particular, we find that miR-9 and miR-132 are able to repress ectopic expression of Foxp2 protein by targeting its 3′ untranslated region (3′UTR) in vivo. Interestingly, ectopic expression of Foxp2 in cortical projection neurons (a scenario that mimics the absence of miRNA-mediated silencing of Foxp2 expression) delays neurite outgrowth in vitro and impairs their radial migration in embryonic mouse neocortex in vivo. Our results uncover a new layer of control of Foxp2 expression that may be required for proper neuronal maturation.

KEY WORDS: MicroRNAs, *Foxp2*, In vivo validation, Mouse

INTRODUCTION

The neocortex of the mammalian brain is a highly organized laminar structure comprising hundreds of different cell types that originates from the development of two embryonic germinal zones: the ventricular zone (VZ) and the subventricular zone (SVZ) of the telencephalon. The VZ and SVZ are composed of distinct but related types of neural progenitor cells (Pinto and Götz, 2007; Fietz and Huttner, 2011; Lui et al., 2011). During cortical development, different subtypes of projection neurons born from neural progenitors migrate out of the germinal zones and cross the intermediate zone (IZ), in an orderly sequence. These neurons accumulate progressively in the cortical plate (CP) to form the six-layered structure of the mammalian neocortex (Molyneaux et al., 2007).

Neuronal subtype specification and migration are finely orchestrated events in developing neocortex (Ayala et al., 2007). To date, several genes and pathways involved in neocortical development have been identified. However, these genes and pathways have been studied individually, leaving it unclear how these different regulators integrate as a network.

In recent years, microRNAs (miRNAs) have rapidly emerged as a new layer of regulation of neocortical development in mammals (Saba and Schratt, 2010). miRNAs are a class of short (~22 nucleotide), non-coding RNAs that control gene expression at the post-transcriptional level, primarily by imperfect base pairing with specific mRNA targets (Krol et al., 2010). The expression patterns and targets of several miRNAs are conserved across chordate evolution, from amphioxus to mammals, suggesting an ancient origin and crucial function in evolutionarily conserved developmental processes (Candiani et al., 2011). Currently, more than 700 miRNAs have been identified in the mouse (http://www.mirbase.org/blog/2011/11/mirbase-18-released/). A unique feature of miRNAs is their ability to regulate many genes in parallel, and in some cases one miRNA can target similar families of genes (Baek et al., 2008; Selbach et al., 2008). Therefore, miRNAs are prime candidates for regulatory molecules that could orchestrate gene networks during complex developmental processes.

To investigate the global function of miRNAs in embryonic mouse neocortex in vivo, recent studies have used depletion of miRNAs by means of genetic inactivation of *Dicer1* (previously *Dicer*), an essential enzyme for the maturation of nearly all miRNAs. However, most of these studies did not lead to the identification of target genes (Makeyev et al., 2007; Choi et al., 2008; De Pietri Tonelli et al., 2008; Kawase-Koga et al., 2009). Other studies have addressed the function of specific miRNAs in embryonic mouse neocortex; however, the identification of targets was often motivated by a gene-specific approach (Arvanitis et al., 2010; Zhao et al., 2009) or in silico predictions (Shibata et al., 2008; Zhao et al., 2010).

It is now well established that miRNAs can also accelerate the decay of target mRNAs, in addition to repressing their translation (Chekulaeva and Filipowicz, 2009; Guo et al., 2010). Therefore, recent studies have used microarrays to identify changes in the expression of potential targets upon manipulation of a single miRNA in cell cultures or in lower vertebrates (Chekulaeva and Filipowicz, 2009; Hendrickson et al., 2009). The identification of putative miRNA targets is only the first step. To validate target genes, the effect of miRNA manipulations on target expression needs to be assessed. Direct regulation of target gene expression by miRNAs has been typically tested by reporter assays. This approach has been mainly used in vitro, and most of these studies perturbed target repression by miRNA overexpression. Therefore, these studies have not provided evidence that physiological levels of miRNA can repress the mRNA target, nor that miRNA-

[1]Department of Neuroscience and Brain Technologies, Fondazione Istituto Italiano di Tecnologia, Via Morego 30, 16163 Genova, Italy. [2]Max-Planck Institute for Evolutionary Anthropology, Deutscher Platz 6, D-04103 Leipzig, Germany. [3]Max-Planck Institute of Molecular Cell Biology and Genetics, Pfotenhauerstrasse 108, D-01307 Dresden, Germany.

*Author for correspondence (davide.depietri@iit.it)

Accepted 18 June 2012

dependent regulation is biologically important (Thomas et al., 2010). For these reasons, the vast majority of targets still await experimental validation (Friedman et al., 2009).

The identification and experimental validation of miRNA target genes is a crucial step towards the identification of miRNA functions. Here, to identify novel miRNA target genes in embryonic neocortex, we depleted miRNAs from the dorsal telencephalon (dTel) of developing mouse embryos and performed gene-expression profiling. We identified a novel miRNA-target gene, *Foxp2*, validated its regulation in vivo and investigated the biological relevance of miRNA-mediated regulation of *Foxp2* with respect to progenitor proliferation, cell-type specification, differentiation and neuronal migration in developing mouse neocortex.

MATERIALS AND METHODS

Mouse lines and in utero electroporation

Mice were housed under standard conditions at the MPI-CBG Dresden (Germany) and IIT Genova (Italy). *Emx1^{Cre}* mice (Iwasato et al., 2000) were crossed with *Dicer^{flox}* mice (Murchison et al., 2005) and genotyped, as previously described (De Pietri Tonelli et al., 2008). Wild-type C57BL/6NCrl females were purchased from Charles River laboratories; vaginal plug day was defined as E0.5. In utero electroporation was performed as previously described (De Pietri Tonelli et al., 2006) with pCAGGS-driven reporter plasmids (each at 1 μg/μl), or in combination with miRNAs inhibitors (Ambion) at final concentration of 25 μM. Embryos were either immediately used (Luciferase assays) or fixed in 4% paraformaldehyde in PBS at 4°C overnight (for immunofluorescence and in situ hybridization). The experiments to investigate the effect of ectopic expression of Foxp2 were initially performed by in utero electroporation of (1:1 ratio) pCAGGS-mCherry/pCAGGS-Foxp2-Δ-3′UTR or (as a control) of pCAGGS-mCherry/pCAGGS-empty plasmids. In case of absence of any relevant phenotype, we did not perform additional controls. This strategy allowed us to 'reduce' the number of animals used in each experiment in accordance with animal-welfare legislations.

Total RNA extraction and microarray analysis

RNA was extracted from the dTel of *Dicer* knockout and control E13.5 embryos with RNeasy kit (Qiagen). Total RNA (5 μg) were labeled, hybridized to Affymetrix Mouse Genome 430 2.0 and scanned following Affymetrix protocols. Data preparation and analysis was conducted in the R statistical environment. Gene-expression levels were analyzed with Affymetrix file using the MG-Mm430 Ensembl Custom CDF file (version 10) based on mouse Ensembl genes. The 'Rma' algorithm was used for background correction and normalization of log2 transformed expression. Genes with expression levels above background were determined based on the Wilcoxon test, with the 'mas5' function (R-Bioconductor 'affy' package) and a cut-off of $P<0.05$. Student's *t*-test was used to compare gene expression levels between the nine samples. The 125 possible permutations of the samples were used to assess significance and FDR (<5%). A list of annotated genes (Ensembl Genes 60) and their statistics is provided in the NCBI GEO database (Accession Number GSE37610). We annotated the biological processes of these genes (Ashburner et al., 2000) using Ensembl Biomart (http://www.ensembl.org/biomart/index.html; Ensembl Genes 60; December 2010). Wilcoxon rank test implemented in FUNC (Prüfer et al., 2007) was used to test the enrichment of high and low ranking t-statistics in *Dicer* knockout samples. Expression values were clustered and visualized using GeneCluster 3.0 and TreeView.

Immunofluorescence and in situ hybridization

Fixed cryosections or vibratome sections (8-40 μm) were prepared as previously described (De Pietri Tonelli et al., 2008). Primary antibodies were used at dilution of 1:500. Mouse monoclonal antibodies were: anti-Cux1 (clone 2A10, Sigma) and anti-Foxp4 (clone 3B12 Abnova, 1:200). Rat monoclonal anti-histone H3 (phospho S28, Abcam) was used. Rabbit polyclonal antibodies were: anti-Foxp2, anti-Foxp4 (1:200) and anti-Tbr2 (Abcam). Goat polyclonal anti-Brn2 (C-20) (Santa Cruz) and guinea-pig polyclonal anti-vGluT1 (Millipore) antibodies were used. Secondary antibodies were from Invitrogen. Detection of Tbr2, Brn2 and Cux1 was performed with antigen retrieval as previously described (De Pietri Tonelli et al., 2008). In situ hybridization was performed as previously described (De Pietri Tonelli et al., 2006; De Pietri Tonelli et al., 2008); sequences of LNA-modified riboprobes (Exiqon) used can be found in supplementary material Table S1. Images were acquired with on Olympus BX61 and Leica TCS SP5 microscopes.

Reporter plasmids

Foxp2 3′UTR, Foxp2, Foxp4, *Renilla*, firefly Luciferases and mCherry-coding regions were PCR amplified and cloned into pCAGGS vector (Niwa et al., 1991). The 3′UTR region of *Foxp2* was cloned downstream of Renilla Luciferase (either in sense or antisense orientation), or downstream of the Foxp2 open reading frame (details available upon request). PCR templates were either BAC clones (BACPAC Resources Center) [RP23-415H10 (*Foxp2*)] or full-length cDNAs clones (Open Biosystems) [BC062926 (*Foxp2*); BC052407 (*Foxp4*)]. Mutations of miR-9 and miR-132 binding-sites in *Foxp2* 3′UTR sequence were achieved using Quick Change Site-Directed Mutagenesis Kit (Stratagene), following the manufacturer's instructions. Sequences of PCR oligonucleotides (Sigma) are available in supplementary material Table S1.

Preparation and morphological analyses of primary cortical neuron cultures

E18.5 mouse embryonic cortices, electroporated in utero at E13.5, were isolated from brains, dissociated by enzymatic digestion with 0.125% trypsin in Neurobasal medium (Invitrogen) for 20 minutes at 37°C and subsequently dissociated mechanically with a fine-tipped Pasteur pipette. The resulting tissue was re-suspended in serum-free Neurobasal medium supplemented with 2% B-27 and 1% Glutamax-I (Invitrogen). Neurons were plated at 600 cells/mm^2 onto poly-D-lysine and laminin (Sigma)-coated glass coverslips (Enzel-Gläser GmbH). Cultures were maintained with antibiotics in Neurobasal medium supplemented with 2% B27 and 1% Glutamax-I for 4 or 7 days. Neurites were analyzed with NeuronJ (Meijering et al., 2004). Sholl analysis (radius step size of 1.85 μm) was performed with ImageJ software (Wayne Rasband, NIH, USA).

Luciferase assays

Embryos were harvested at the indicated times after in utero electroporation. Brains were homogenized in 600 μl of PLB (Promega) at 4°C using a SilentCrusher S (Heidolph) and centrifuged for 10 minutes at 10,600 ***g*** at 4°C prior to Luciferase measurements. Data are the mean of at least seven brains (or pools of two brains each), obtained from at least three pregnant females. Luciferase assays were performed with DLR assay system (Promega) using a Victor3-V luminometer (PerkinElmer).

Quantification and statistical analyses

Phosphohistone-H3- (or Tbr2-) mCherry double-positive cells were quantified in embryonic cortices in the VZ/SVZ (determined as the region of the cortical wall between the upper edge of the Tbr2-positive staining and the ventricle boundary) and neuronal layers (determined by subtracting VZ/SVZ from the entire cortical wall) in each field (40× objective) and expressed as a proportion of total mCherry$^+$ cells. The number of mCherry$^+$ cells in the intermediate zone (IZ) of targeted brains was expressed as percent of total mCherry$^+$ cells per field (20× objective). The IZ was determined as the region between layer VI (Foxp2 positive) and SVZ. mCherry$^+$ cells were counted across representative fields of the electroporated postnatal cortices. Distribution of mCherry-positive neurons, or mCherry-Cux1 and mCherry-Brn2 double-positive neurons were quantified in each of 10 or five bins, respectively (three to five brain were counted per condition; three to five sections along the rostrocaudal axis were counted per brain) and overly conservative Bonferroni correction was applied. Eleven to 150 neurons per condition (four independent preparations) were analyzed for quantification. Data are expressed as mean±s.e.m. for all quantifications and assays. Unless stated otherwise, two-tailed Student's *t*-tests were performed and differences considered to be significant when $P<0.05$.

RESULTS

Foxp2 is prematurely expressed in the embryonic neocortex of *Dicer* knockout mice

In our previous study, to investigate the role of miRNAs in embryonic mouse neocortex, we depleted mature miRNAs in the dTel of developing mouse embryos by mean of genetic ablation of *Dicer*. This was carried out by crossing *Dicer*^{flox} mice with *Emx1*^{Cre} mice, which express the Cre-recombinase in the neural progenitors of the dTel starting from embryonic day 9.5 (E9.5) (De Pietri Tonelli et al., 2008). Here, we used the same genetic approach to deplete miRNAs, but we applied a genome-wide expression analysis using oligonucleotide microarrays to identify novel miRNA target genes in embryonic mouse neocortex. Among the 12,198 Ensembl genes detected above background (out of the 15,758 present on the array), we found 3027 differently expressed in dTel of E13.5 *Dicer* knockout mouse embryos (*Dicer*$^{flox/flox}$ *Emx1*$^{Cre/wt}$, Fig. 1A, supplementary material Fig. S1) compared with control littermates (*Dicer*$^{flox/wt}$ *Emx1*$^{Cre/wt}$, Fig. 1A, supplementary material Fig. S1), at a false discovery rate (FDR) threshold of 5%. Among the genes upregulated in dTel of *Dicer* knockout mice, the ten most common gene-ontology (GO) categories were mainly related to signaling and developmental processes (Wilcoxon rank test, $P<2\times10^{-16}$) (supplementary material Fig. S1A). These categories also included 'Gene silencing by RNAi', a group containing *Dicer* itself, *Dgcr8*, *Adar* and *Lin28*, genes that encode regulators of miRNA processing, as well as *Mov10*, *Tnrc6a* and *Tnrc6b*, which encode for effectors of miRNA activity (Krol et al., 2010). This finding suggests a potential feedback process upon depletion of mature miRNAs. By contrast, among the downregulated genes, the ten most common GO categories were related to metabolic functions (supplementary material Fig. S1B). This could reflect the progressive decrease in progenitor proliferation that we previously observed in the dTel of *Dicer* knockout mouse embryos (De Pietri Tonelli et al., 2008). Interestingly, considering only the 62 genes with the biggest modulation (a greater than twofold change), 51/62 were upregulated in dTel of *Dicer* knockout embryos (Fig. 1A; supplementary material Fig. S1C). This bias towards upregulated genes potentially reflects an enrichment of miRNA targets. Indeed, several known miRNA targets such as *Olig2*, *Tac1*, *Tnc*, *Rasgrp1* and *Camta1* were among the upregulated genes (Fig. 1A; supplementary material Fig. S1C). By contrast, no previously known miRNA targets were present among the downregulated genes. A particularly interesting candidate upregulated gene was *Foxp2* (Fig. 1A; supplementary material Fig. S1C). *Foxp2* is a member of the Forkhead-box family of transcription factors. Two functional copies of this transcription factor are required for the proper development of speech and language in humans (Fisher and Scharff, 2009; Lai et al., 2001), and two amino acid changes during human evolution might have tuned specific speech-relevant properties of corticobasal ganglia circuits (Enard, 2011; Enard et al., 2009; Enard et al., 2002). In the embryonic mouse, neocortex Foxp2 starts its expression in postmigratory neurons, and in the postnatal cortex it is restricted to projections neurons of layers V-VI (Ferland et al., 2003; Takahashi et al., 2003; Campbell et al., 2009; Hisaoka et al., 2010; Reimers-Kipping et al., 2011). Remarkably, detectable levels of *Foxp2* mRNA have been reported in embryonic germinal zones of the mouse telencephalon – but not Foxp2 protein (Ferland et al., 2003; Takahashi et al., 2003). Additionally, the 3′UTR of *Foxp2* mRNA is highly conserved among vertebrates and contains multiple predicted miRNA-binding sites (supplementary material Fig. S2). These data suggest that *Foxp2* expression might be regulated by miRNAs in the embryonic neocortex.

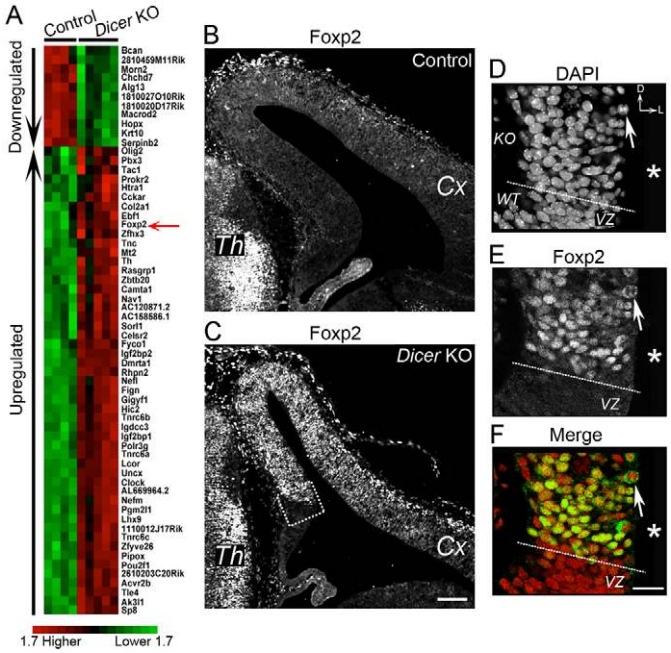

Fig. 1. *Foxp2* is prematurely expressed in the embryonic neocortex of *Dicer* knockout mice. (**A**) Microarray analysis of total RNA from dorsal telencephalon (dTel) of E13.5 control (*Dicer*$^{flox/wt}$ *Emx1*$^{Cre/wt}$; *n*=4) and conditional *Dicer* knockout (*Dicer* knockout; *Dicer*$^{flox/flox}$ *Emx1*$^{Cre/wt}$; *n*=5) littermate mouse embryos. Black arrows indicate either down- or upregulated genes; red arrow indicates *Foxp2*. (**B-F**) Immunoflorescence with anti-Foxp2 antibody in the dTel of E13.5 control (B) and *Dicer* knockout (C-F) littermate embryos, counterstained for DNA with DAPI (D,F). Dashed box in C indicates a region similar to the one shown in D-F. Arrows indicate ectopic Foxp2 expression in a neural progenitor cell of *Dicer* knockout region (D-F, above the dotted line). Asterisks indicate the lumen of the lateral ventricle. Th, thalamus; Cx, cortex; *VZ*, ventricular zone. Section orientation is indicated in D. D, dorsal; L, lateral. Scale bars: 100 μm in B,C; 25 μm in D-F.

To test whether the two- to sevenfold increase in *Foxp2* mRNA expression observed upon miRNA depletion (Fig. 1A) is paralleled by an increase in *Foxp2* protein, we performed immunofluorescence detection of endogenous Foxp2 protein in the brain of E13.5 *Dicer* knockout embryos (Fig. 1C-F). Consistent with previous reports (Ferland et al., 2003; Lai et al., 2003; Takahashi et al., 2003), Foxp2 protein was expressed in the thalamus of both control and *Dicer* knockout brains at E13.5 (Fig. 1B,C). However, consistent with the array data, Foxp2 protein was prematurely expressed in the dTel of *Dicer* knockout embryos (the region in which *Emx1*-driven Cre expression triggers genetic inactivation of *Dicer*) (De Pietri Tonelli et al., 2008) (Fig. 1C) and also in some neural progenitors of the VZ (Fig. 1D-F). The expression pattern of Foxp2 in the dTel of Dicer knockout embryos probably reflected the expression pattern of *Emx1* gene, which has a high medial-to-lateral gradient (Simeone et al., 1992; Nakagawa et al., 1999; Muzio et al., 2002). The premature expression of endogenous Foxp2 protein in miRNA-depleted embryonic neocortex raises the possibility that expression of *Foxp2* is directly controlled by miRNAs in this tissue.

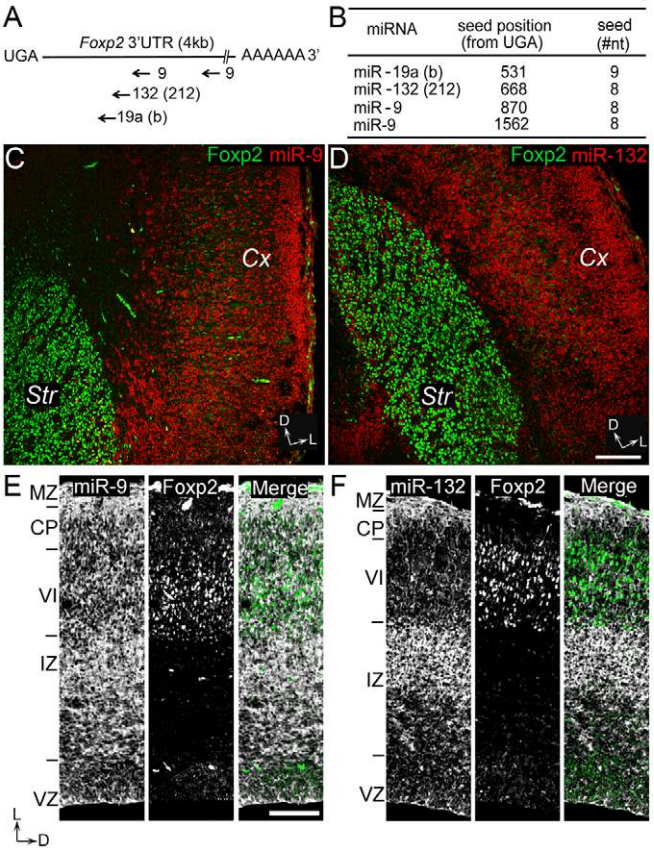

Fig. 2. *Foxp2* is a putative target of miR-9 and miR-132. (**A**) Candidate miRNAs (arrows) and their predicted binding position in *Foxp2* 3′UTR (broken line) are shown. (**B**) Predicted position of binding sites of each candidate miRNA into mouse *Foxp2* 3′UTR, and number of predicted nucleotides in the seed. (**C-F**) In situ hybridization for mature miR-9 (C, red; E, white) or mature miR-132 (D, red; F, white), and immunofluorescence staining with anti-Foxp2 antibody (C-F, green) in the dTel of E18.5 wild-type mouse embryos. Cx, cortex; Str, striatum; MZ, marginal zone, CP, cortical plate; VI, layer VI; IZ, intermediate zone; VZ, ventricular zone. Section orientation is indicated. D, dorsal; L, lateral. Scale bars: 100 μm.

Foxp2 is a putative target of miR-9 and 132

To investigate whether Foxp2 expression is controlled by miRNAs, we performed in silico (Fig. 2A,B) and in situ (Fig. 2C-F) analyses. Several miRNAs have predicted binding sites in *Foxp2* 3′UTR (supplementary material Fig. S2). We restricted the number of candidate miRNAs by considering only brain-expressed miRNAs with binding sequences that are conserved in chick, mouse, rat and human *Foxp2* 3′UTR, and that are predicted by TargetScan, MicroCosm targets and mirSVR databases (Betel et al., 2010; Griffiths-Jones et al., 2008; Lewis et al., 2005). Using these criteria, we found two predicted binding sites for miR-9, a brain-specific miRNA abundantly expressed in the developing mammalian brain; one predicted binding site for the brain-enriched miR-132; and one predicted binding site for miR-19, which is moderately expressed in brain (Lagos-Quintana et al., 2002) (Fig. 2A,B). To correlate their expression patterns with that of endogenous Foxp2 protein in the telencephalon of wild-type mice, we performed *in situ* hybridization using locked-nucleic-acid-modified (LNA) probes for mature miR-19b (not shown), miR-9 (Fig. 2C,E) and miR-132 (Fig. 2D,F), combined with immunofluorescence detection of Foxp2 protein (Fig. 2C-F). This experiment was performed at E18.5, when Foxp2 protein expression in the embryonic neocortex is clearly detectable. Expression pattern of miR-19b was widespread throughout developing brain (not shown). By contrast, the expression of miR-9 and miR-132 was enriched in the dTel (where Foxp2 protein expression is low; Fig. 2C,D) and was low or undetectable in the striatum (where Foxp2 protein expression is abundant; Fig. 2C,D). Within the dTel, the expression of miR-9 was widespread throughout the lateral cortex and only partially overlapping with the Foxp2-positive layers (Fig. 2E), whereas miR-132 expression was enriched in the IZ and less abundant or undetectable in the Foxp2-positive layers (Fig. 2F). These results are compatible with a possible function of miR-9 and miR-132 in the control of Foxp2 expression in embryonic neocortex.

Foxp2 3′UTR can yield post-transcriptional repression of Luciferase in embryonic neocortex

Previous studies have demonstrated that miRNAs repress gene expression by binding preferentially to the 3′UTR of target mRNAs (Arvanitis et al., 2010; Guo et al., 2010; Lai, 2002). To investigate whether the 3′UTR of *Foxp2* mRNA is susceptible to post-transcriptional repression in embryonic mouse neocortex, we performed Luciferase assays in vivo (Fig. 3). We fused mouse *Foxp2* 3′UTR downstream to *Renilla* Luciferase (Rluc), either in sense orientation (pCAGGS-Rluc-Foxp2-3′UTR-WT, Fig. 3A) or, as a control, in antisense orientation (pCAGGS-Rluc-Foxp2-3′UTR-AS, Fig. 3A). We delivered these reporter plasmids to a spatiotemporally restricted population of VZ neural progenitors (and their progeny) in the dTel of E13.5 wild-type mouse embryos, using in utero electroporation (Saito and Nakatsuji, 2001). In addition to the Rluc reporter plasmid, in this and subsequent Luciferase experiments we also delivered a plasmid expressing firefly Luciferase (Fluc, pCAGGS-Fluc, Fig. 3A), which allowed us to account for variations in transfection efficiency, along with a plasmid expressing a red fluorescent protein, which was used to identify the targeted cells (pCAGGS-mCherry, Fig. 3A). Consistent with previous reports (De Pietri Tonelli et al., 2006; Langevin et al., 2007), analysis of fluorescence in electroporated brains 8, 48 or 4 days after electroporation confirmed that expression of mCherry was restricted to the population of targeted neural progenitors in VZ/SVZ (Fig. 3B), or was located in both targeted progenitors and neurons that were generated by them (Fig. 3C), or mostly in neurons that reached neuronal layers (Fig. 3D), respectively. We then quantified the expression of Rluc and Fluc in the electroporated dTel by measuring their enzymatic activity. We observed a significant decrease in expression of Rluc when *Foxp2* 3′UTR (in sense orientation) was fused downstream of Rluc, at all the time points (Fig. 3E-G). These results are compatible with a miRNA-dependent repression of Foxp2 3′UTR in both progenitor cells and neurons of the embryonic neocortex.

Endogenous miR-9 and miR-132 repress Luciferase by targeting *Foxp2* 3′UTR in embryonic neocortex

Fig. 2 shows that *Foxp2* is a putative target of miR-9 and miR-132. We investigated whether these miRNAs target *Foxp2* 3′UTR (Fig. 4) in vivo by using specific antisense inhibitors to block their activity. miR-9 is expressed throughout the lateral cortex (Fig. 2F) and has a strong pro-neurogenic function in progenitor cells (Yuva-Aydemir et al., 2011). miR-132 expression is enriched in the IZ (Fig. 2F) and is known to control various aspects of neuronal maturation (Hansen et al., 2010; Lambert et al., 2010; Magill et al., 2010; Olde Loohuis et al., 2011). Inhibition of miR-9 may interfere

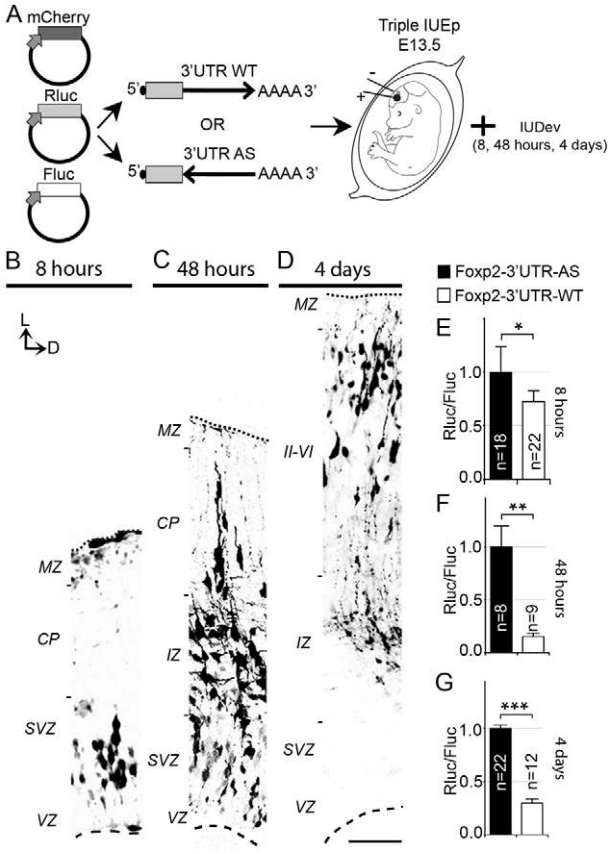

Fig. 3. *Foxp2* 3′UTR can yield post-transcriptional repression of Luciferase in embryonic neocortex. (**A**) CAG promoter-driven plasmids express mCherry (pCAGGS-mCherry), *Renilla* Luciferase (Rluc, pCAGGS-Rluc) or firefly luciferase (Fluc, pCAGGS-Fluc). The wild-type (WT) 3′UTR of *Foxp2* was inserted downstream of Rluc in sense (pCAGGS-Rluc-Foxp2-3′UTR-WT) or antisense orientation (pCAGGS-Rluc-Foxp2-3′UTR-AS, control). In utero electroporation was used to deliver plasmids in the neural progenitors of dorsal telencephalon (dTel) of E13.5 wild-type embryos. Embryos were allowed to develop in utero (IUDev) for the indicated times. (**B-D**) Fluorescence images of cryosections through cortices of mouse embryos, electroporated with pCAGGS-mCherry, pCAGGS-Fluc and pCAGGS-Rluc-Foxp2-3′UTR-WT and developed for the indicated times, showing targeted cells (mCherry positive) confined in ventricular zone (VZ) and sub-ventricular zone (SVZ) in B, or in both VZ/SVZ and intermediate zone (IZ) in C or in layers II-VI in D. Dotted lines indicate pial surface. Dashed lines indicate ventricular surface. MZ, marginal zone; CP, cortical plate; II-VI indicate the cortical layers. Section orientation is indicated. D, dorsal; L, lateral. Scale bar: 100 μm. (**E-G**) Rluc/Fluc ratio measured in lysates of brains electroporated as in B-D. Black bars, pCAGGS-Rluc-Foxp2-3′UTR-AS; white bars, pCAGGS-Rluc-Foxp2-3′UTR-WT. Rluc/Fluc ratio of pCAGGS-Rluc-Foxp2-3′UTR-AS samples was normalized to one. *n*, number of brains (or pool of two brains) analyzed per condition. **P*<0.05; ***P*<0.01; ****P*<0.001.

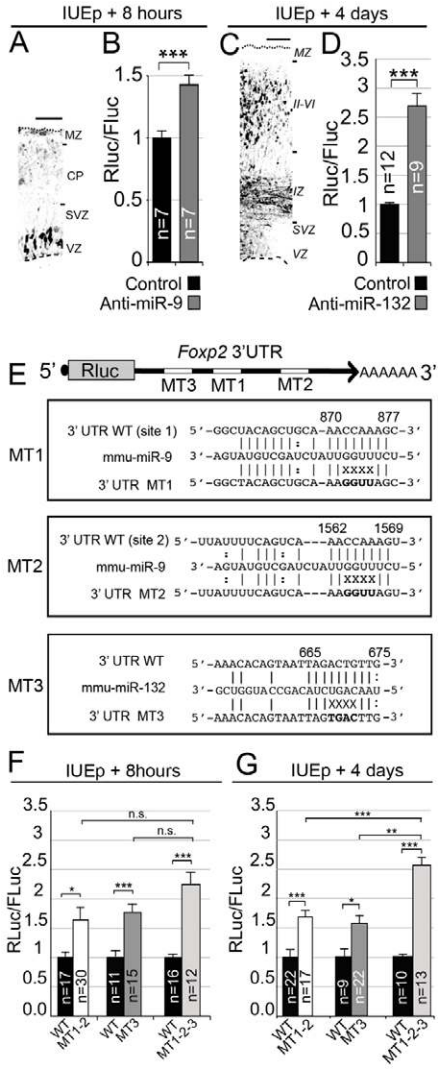

Fig. 4. Endogenous miR-9 and miR-132 repress Luciferase by targeting *Foxp2* 3′UTR in embryonic neocortex. (**A**,**C**) Images of cryosections through the dTel of embryos electroporated at E13.5 (as in B,D) and developed in utero for the indicated time, illustrating intrinsic mCherry fluorescence. MZ, marginal zone; CP, cortical plate; II-VI indicate the cortical layers; VZ, ventricular zone; SVZ, sub-ventricular zone. Dotted lines indicate the pial surface; dashed lines indicate the ventricular surface. Scale bars: 50 μm. (**B**,**D**) Rluc/Fluc ratio measured in brain lysates from wild-type mouse embryos co-electroporated with pCAGGS-mCherry, pCAGGS-Fluc, pCAGGS-Rluc-Foxp2-3′UTR-WT, and either scrambled (B,D, control, black bar), miR-9 inhibitor (B, anti-miR-9, gray bar) or miR-132 inhibitor (D, anti-miR-132, gray bar), and developed in utero for the indicated time. Rluc/Fluc ratio of control samples was normalized to one. ****P*<0.001. (**E**) Predicted binding sites of miR-9 (mmu-miR-9) and miR-132 (mmu-miR-132) in *Foxp2* 3′UTR (3′UTR WT). Four nucleotides (bold) were mutated in each of the putative binding sites of miR-9 (3′UTR MT1 and MT2) or of miR-132 (3′UTR MT3). Vertical lines indicate putative base pairings; columns indicate G-U bindings; 'X' indicates a mismatch. (**F**,**G**) Rluc/Fluc ratio measured in brain lysates from wild-type mouse embryos co-electroporated in utero at E13.5 with pCAGGS-mCherry, pCAGGS-Fluc, and either pCAGGS-Rluc-Foxp2-3′UTR-WT (black bars), pCAGGS-Rluc-Foxp2-3′UTR-MT1-2 (white bars), pCAGGS-Rluc-Foxp2-3′UTR-MT3 (dark gray bars) or pCAGGS-Rluc-Foxp2-3′UTR-MT1-2-3 (light gray bars), and developed in utero for the indicated time. Rluc/Fluc ratio of pCAGGS-Rluc-Foxp2-3′UTR-WT samples was normalized to one. One-way analysis of variance (ANOVA) was used for statistical analysis. **P*<0.05; ***P*<0.01; ****P*<0.001; n.s., not significant.

with neurogenesis, whereas inhibition of miR-132 may interfere with neuronal maturation. We used in utero electroporation to deliver synthetic antisense inhibitors specific for miR-9 (Fig. 4A,B), miR-132 (Fig. 4C,D) or scrambled control (Fig. 4B,D), along with pCAGGS-Rluc-Foxp2-*3′UTR*-WT (see Fig. 3A), in the dTel of E13.5 wild-type mouse embryos. To avoid interferences with neurogenesis, we examined the effect of miR-9 inhibition on

Foxp2 3′UTR in progenitors (8 hours after electroporation, Fig. 4A). Conversely, given the enriched expression of miR-132 in the IZ, we analyzed the effect of miR-132 inhibition on Foxp2 3′UTR in neurons (4 days after electroporation, Fig. 4C). We then quantified the expression of Rluc and Fluc in the electroporated dTel by measuring their enzymatic activity (Fig. 4B,D). We observed a significant rescue of Rluc expression upon administration of miR-9 or miR-132 inhibitors. This experiment shows that endogenous miR-9 and miR-132 repress Luciferase by targeting the *Foxp2* 3′UTR in progenitors and neurons, respectively. Cortices electroporated with either mir-9 or miR-132 inhibitors were further analyzed by immunofluorescence for the expression of endogenous Foxp2 protein; however, under these conditions we did not detect an increased expression of the endogenous Foxp2 protein in targeted cells (data not shown). The lack of de-repression of the endogenous Foxp2 expression may be due to insufficient inhibition of the endogenous miR-9/132 (which are very abundant in embryonic neocortex), to progressive dilution of the synthetic miRNA inhibitors in proliferating progenitors or to a redundant action of additional miRNAs on Foxp2.

Next, we wanted to validate experimentally the predicted binding sequences of miR-9 and miR-132 within *Foxp2* 3′UTR in the embryonic neocortex. Previous studies have shown that miRNA-target interaction occurs mostly by formation of base pairing between the 5′ region of the miRNA (seed) with its target (Brennecke et al., 2005; Lewis et al., 2005). We therefore prepared plasmids in which, downstream of Rluc, we fused a mutated 3′UTR of *Foxp2* in which sequences assumed to base pair with miR-9 or miR-132 (or both) were altered (Fig. 4E). Using this strategy, we also aimed to investigate the activity and relative efficiency of miR-9 and miR-132 for the repression of Foxp2 3′UTR in both progenitors and neurons. We used in utero electroporation to deliver each mutated plasmid (Fig. 4E) into the dTel of E13.5 wild-type mouse embryos. As a control, we electroporated pCAGGS-Rluc-Foxp2-3′UTR-WT (see Fig. 3A). We then quantified Luciferase expression in neural progenitors in VZ/SVZ (Fig. 4F) and in neurons in the neuronal layers (Fig. 4G). Mutations that prevented the binding of *either* endogenous miR-9 or miR-132 to *Foxp2* 3′UTR rescued Rluc expression in both progenitors (Fig. 4F) and neurons (Fig. 4G). Remarkably, mutations that affected the binding of *both* miR-9 and miR-132 resulted in an additive rescue of Rluc expression in neurons, but not in progenitors (Fig. 4F,G). These results are consistent with the natural expression patterns of miR-9 and of miR-132 (Fig. 2) (De Pietri Tonelli et al., 2008; Shibata et al., 2011) and suggest that the activity of these miRNAs can converge on Foxp2-3′UTR in neurons.

Ectopic expression of Foxp2 in neural progenitors does not impair their subtype specification and differentiation in embryonic neocortex

To investigate the possible biological relevance of the miRNA-mediated repression of Foxp2-3′UTR in the embryonic neocortex, we ectopically expressed Foxp2 protein in neural progenitors (a scenario that mimics the absence of miRNA-mediated silencing of Foxp2 expression) and investigated the consequences on cell-type specification and differentiation. Progenitors that divide in the SVZ (also known as basal progenitors) are generated from progenitors that divide in the VZ (also known as apical progenitors), and can be identified by the expression of the transcription factor *Tbr2* (*Eomes*) (Englund et al., 2005). We used in utero electroporation to deliver the pCAGGS-mCherry plasmid into the dTel of E13.5 wild-type mouse embryos, along with either pCAGGS empty plasmid (control), or a plasmid expressing a transcript encoding Foxp2 protein lacking its 3′UTR, so that it could not be targeted by miR-9 and miR-132 (pCAGGS-Foxp2-Δ-3′UTR) (supplementary material Fig. S3A-C). Immunofluorescence analysis with anti-Foxp2 antibody 24 hours after electroporation revealed that almost all (96±4%) targeted cells in the VZ/SVZ that expressed mCherry also expressed Foxp2 protein (supplementary material Fig. S3A-C). Therefore, in subsequent experiments, cells expressing mCherry were also considered positive for Foxp2 protein when the latter was co-electroporated. We next compared the cortices that ectopically expressed Foxp2 with those not expressing ectopic Foxp2 40 hours after electroporation (supplementary material Fig. S3D-J). Quantification of the proportion of apical progenitors (Tbr2-negative mCherry-positive cells) and of basal progenitors (Tbr2 and mCherry double-positive cells) revealed no difference between the two conditions (supplementary material Fig. S4J). Similarly, we found no difference in the proportion of targeted progenitors undergoing basal and apical mitoses (identified by co-expression of mCherry and of the mitotic marker phosphohistone H3) (not shown). Finally, we quantified the number of cells generated by targeted progenitors, that delaminated from the VZ/SVZ (i.e. mCherry-positive cells that were located in neuronal layers) and again we found no difference between the two conditions (supplementary material Fig. S4D,G,K). These results indicate that progenitor subtype specification or differentiation is not impaired after ectopic Foxp2 expression.

Ectopic Foxp2 expression impairs radial migration of targeted cells in embryonic neocortex, by a miR-9/132-dependent mechanism

In the embryonic mouse neocortex, Foxp2 starts its expression in postmigratory neurons (Ferland et al., 2003; Takahashi et al., 2003). Endogenous miR-9 and miR-132 repressed Luciferase expression by targeting Foxp2 3′UTR in neurons of the embryonic neocortex (Fig. 4), raising the possibility that this control may be important for neuronal migration or maturation. To test this hypothesis, we used in utero electroporation to deliver the pCAGGS-mCherry plasmid into the dTel of E13.5 wild-type mouse embryos, along with (1) pCAGGS empty plasmid (control, Fig. 5A,B), (2) pCAGGS-Foxp2-Δ-3′UTR (Fig. 5C,D), (3) pCAGGS-Foxp2-3′UTR-MT1+2+3 [expressing a transcript for the *Foxp2*-coding sequence and a mutated 3′UTR (as in Fig. 4) that is not targeted by miR-9 and miR-132 (Fig. 5E,F)] or (4) pCAGGS-Foxp2-3′UTR-WT [expressing a transcript for *Foxp2*-coding sequence and its WT 3′UTR (Fig. 5G,H)]. Five days after electroporation, we first examined the expression of Foxp2 protein in electroporated cortices (Fig. 5B,D,F,H). Immunoreactivity of Foxp2 protein in control cortices (Fig. 5B) was consistent with previous studies (Ferland et al., 2003; Shu et al., 2001; Takahashi et al., 2003) and comparable with the expression of Foxp2 protein in cortices electroporated with the Foxp2 construct carrying wild-type 3′UTR (Fig. 5H). By contrast, immunoreactivity of Foxp2 protein was strongly increased in cortices electroporated with the Foxp2 construct lacking the 3′UTR (Fig. 5D), as well as in cortices electroporated with the Foxp2 construct carrying a mutated 3′UTR in miR-9/132 binding sites (Fig. 5F). We next analyzed the distribution of targeted cells in cortex. We found comparable distributions of targeted cells in control cortices and in cortices electroporated with pCAGGS-Foxp2-3′UTR-WT (Fig. 5A,G,I), consistent with previous studies (De Pietri Tonelli et al., 2006; Langevin et al., 2007). By contrast, in cortices electroporated with pCAGGS-Foxp2-Δ-3′UTR and pCAGGS-Foxp2-3′UTR-MT1+2+3, we found that many of the targeted cells were misplaced

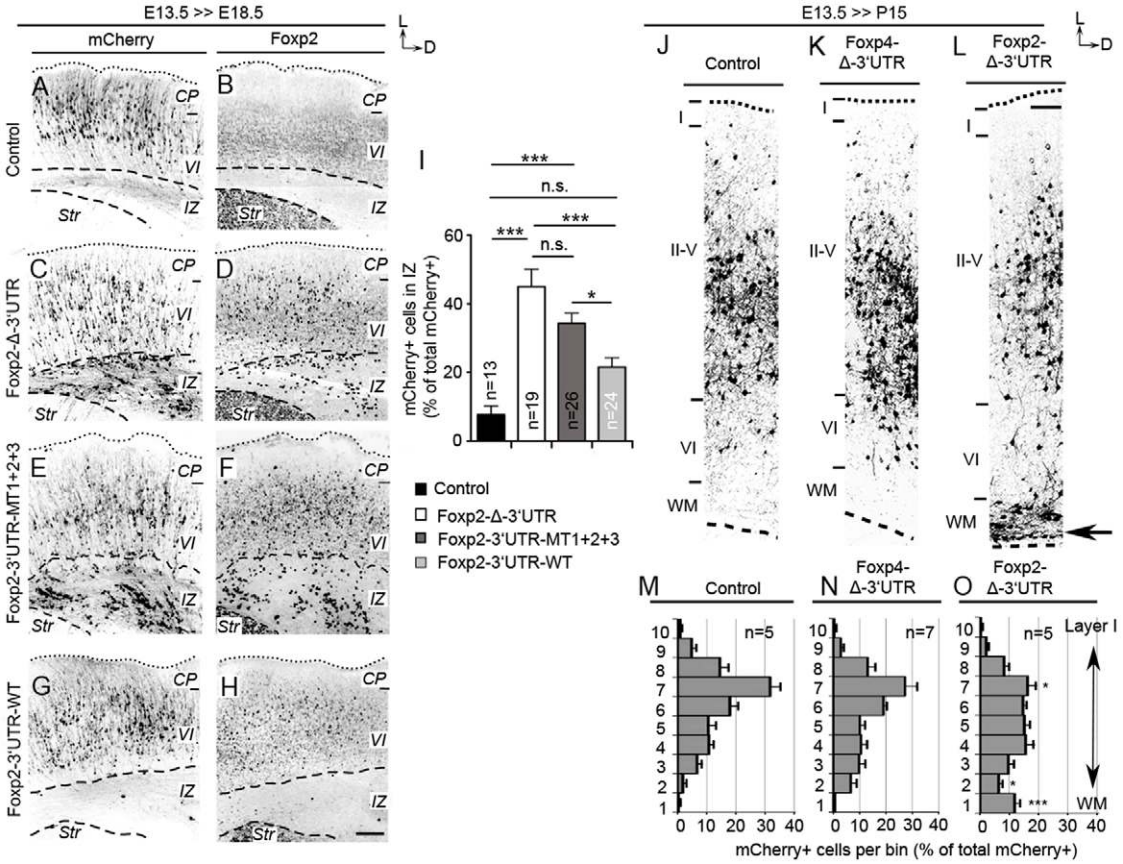

Fig. 5. Ectopic Foxp2 expression impairs radial migration of targeted cells in embryonic neocortex, by a miR-9/132-dependent mechanism. (**A-H**) Images of cryosections through the telencephalon of E18.5 wild-type mouse embryos co-electroporated in utero at E13.5 with pCAGGS-mCherry along with either pCAGGS (control) (A,B), pCAGGS-Foxp2-Δ-3′UTR (C,D), pCAGGS-Foxp2-3′UTR-MT1+2+3 (E,F) or pCAGGS-Foxp2-3′UTR-WT (G,H), showing intrinsic fluorescence of mCherry (A,C,E,G) or Foxp2 immunostaining (B,D,F,H). CP, cortical plate; VI, layer VI; Str, striatum. Dashed lines indicate the limits of the intermediate zone (IZ). Scale bar: 50 μm. (**I**) Quantification of the proportion of targeted cells located in the IZ of the electroporated cortices per field (as shown in A,C,E,G). One-way analysis of variance (ANOVA) was used for statistical analysis. *n*, number of sections counted across rostrocaudal axes from at least four brains per condition. Data are mean±s.e.m. (**J-L**) Images of sections through the cerebral cortex of postnatal day 15 (P15) wild-type mice co-electroporated in utero at E13.5 with pCAGGS-mCherry and either pCAGGS (J, control), pCAGGS-Foxp4-Δ-3′UTR (K, Foxp4-Δ-3′UTR) or pCAGGS-Foxp2-Δ-3′UTR (L, Foxp2-Δ-3′UTR), showing intrinsic mCherry fluorescence. Arrow indicates ectopic cells in the white matter (WM); dashed lines indicate the bottom limit of WM; I-VI indicate cortical layers. Orientation of sections is indicated. D, dorsal; L, lateral. Scale bar: 100 μm. Dotted lines in A-H,J-L indicate pial surface. (**M-O**) Quantification of the proportion of mCherry-positive cells located in each of the 10 bins per field (as in J-L) along the rostrocaudal axis, counted from at least five brains per condition; n.s., non significant. P=0.1; *P<0.05, ***P<0.001. Data are mean±s.e.m.

in the IZ (Fig. 5C,E,I). These results show that ectopic expression of Foxp2 protein impairs radial migration of neurons, and that this effect on migration is attenuated by the repressive action of endogenous miR-9/132 on Foxp2 3′UTR in the embryonic neocortex.

We then asked whether the misplaced cells were delayed or arrested in their migration. To discriminate between these two possibilities, electroporated cortices were analyzed at postnatal day 15 (P15), when neuronal migration is largely complete (Fig. 5J-O). To exclude possible artifacts owing to the ectopic expression of a transcription factor, we used Foxp4 as an additional control. *Foxp4* is the closest paralog of *Foxp2*, and in the embryonic mouse neocortex Foxp4 protein is co-expressed with Foxp2 and interacts with it (Li et al., 2004; Takahashi et al., 2008). Cortices were electroporated at E13.5 with pCAGGS-mCherry plasmid along with (1) pCAGGS empty plasmid (Fig. 5J,M), (2) pCAGGS-Foxp4-Δ-3′UTR [expressing a transcript for *Foxp4* lacking the 3′UTR (to avoid eventual post-transcriptional effects) (Fig. 5K,N)] or (3) pCAGGS-Foxp2-Δ-3′UTR (Fig. 5L,O). At P15 we analyzed the laminar distribution of targeted cells. Laminar distribution of cells in control cortices (Fig. 5J,M) and in cortices electroporated with the Foxp4 construct was comparable (Fig. 5K,N; immunofluorescent verification of Foxp4 expression not shown). By contrast, in cortices electroporated with the Foxp2 construct, a greater proportion of cells were located in deeper cortical layers, and some were also found in the white matter (Fig. 5L,O). This finding corroborates the results of the previous experiment (Fig. 5A-I) and suggests that ectopic expression of Foxp2 protein in embryonic neocortex arrests radial migration of some targeted cells.

Ectopic expression of Foxp2 delays neurite outgrowth and branching in cortical neurons

To investigate whether ectopic expression of Foxp2 protein can impair the differentiation of cortical projection neurons, we briefly examined the cells after ectopic Foxp2 expression in P15 brains (as

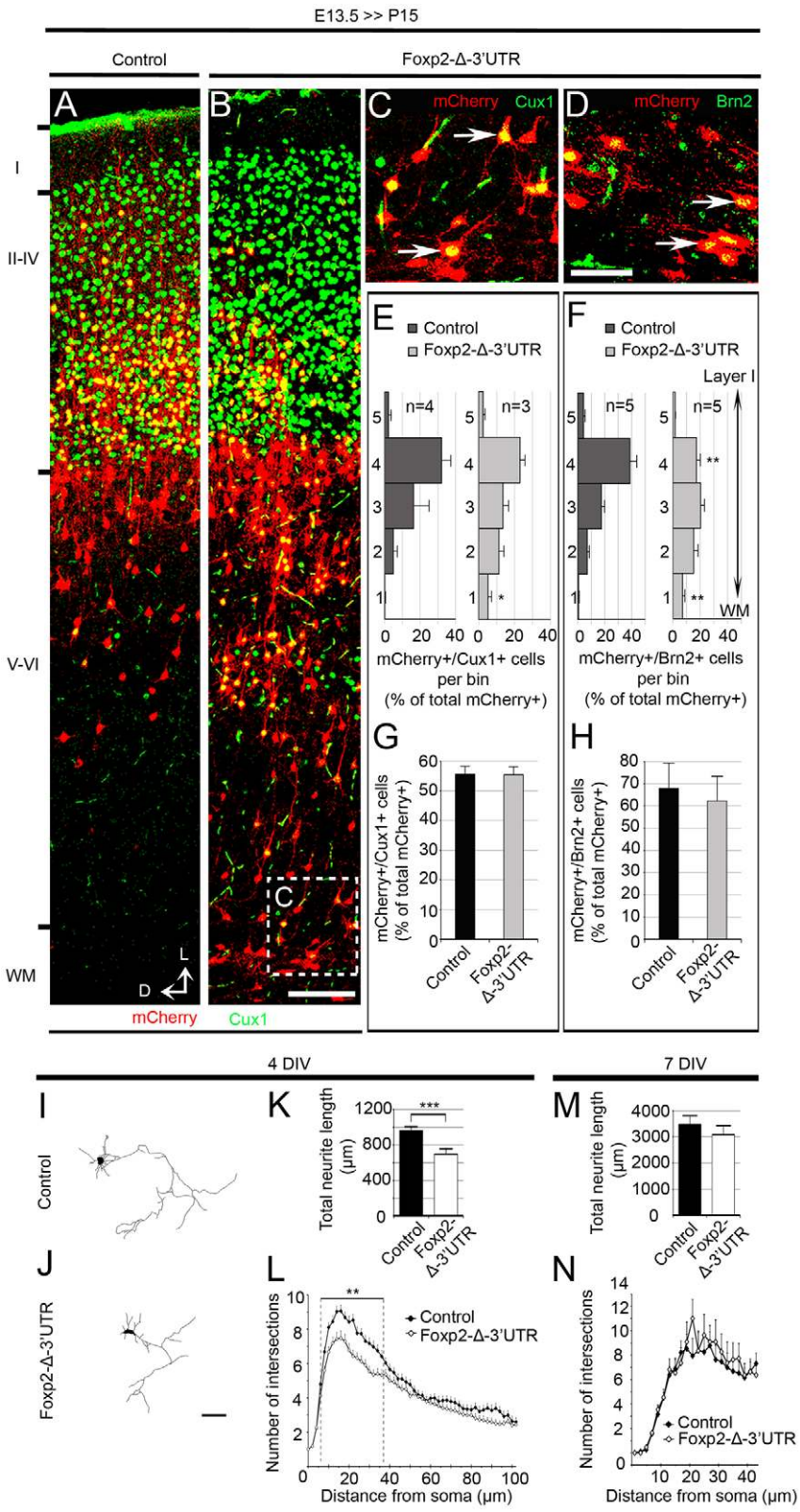

Fig. 6. Ectopic expression of Foxp2 delays neurite outgrowth and branching in cortical neurons. (**A-D**) Images of sections through the cerebral cortices of wild-type P15 mice, co-electroporated in utero at E13.5 with pCAGGS-mCherry and either pCAGGS (A) or pCAGGS-Foxp2-Δ-3′UTR (B-D), showing intrinsic fluorescence of mCherry (A-D, red) and Cux1 (A-C, green) or Brn2 (D, green). Dashed box in B indicates a region similar to the ones shown in C and D. Arrows indicate mCherry-Cux1 (C) or mCherry-Brn2 (D) double-positive neurons. Scale bars: 100 μm in A,B; 50 μm in C,D. (**E**,**F**) Quantification of the distribution of mCherry-Cux1 (E) or mCherry-Brn2 (F) double-positive neurons in the cortical wall (divided in five bins along the dorsoventral axis) per field (as in A,B). (**G**,**H**) Quantification of the relative proportion of mCherry-Cux1 (G) or mCherry-Brn2 (H) double-positive neurons among the entire population of targeted cells (mCherry positive) per field (as in A,B). WM, white matter; I-VI indicate cortical layers. Section orientations are indicated. D, dorsal; L, lateral. (**I**,**J**) Representative tracings of primary cortical projection neurons from E18.5 wild-type mouse embryos co-electroporated in utero at E13.5 with pCAGGS-mCherry and either pCAGGS (I, control) or pCAGGS-Foxp2-Δ-3′UTR (J, Foxp2-Δ-3′UTR) and cultivated in vitro for 4 days (4 DIV). Scale bar: 15 μm. (**K-N**) Quantification of total neurite length (K,M) and branching (L,N) of mCherry-positive primary cortical projection neurons from control embryos (control, black bars in K,M; black diamonds in L,N) or co-electroporated with pCAGGS-Foxp2-Δ-3′UTR (white bars, K,M; white diamonds in L,N) and cultivated for 4 days in vitro (K,L) or 7 days in vitro (M,N). In E-H,K-N, data are mean±s.e.m. **P*<0.05; ***P*<0.01; ****P*<0.001.

in Fig. 5L). At the morphological level, cells arrested in the white matter exhibited a tangential morphology and some of them extended processes; moreover, some of these cells acquired glutamatergic fate (supplementary material Fig. S4). We also stained the electroporated cortices (as in Fig. 5J,L) for Cux1 (Fig. 6A-C) or Brn2 (also known as *Pou3f2*, Fig. 6D) protein, which are markers of cortical projection neurons of the upper layers (Molyneaux et al., 2007). We analyzed the distribution of targeted neurons (mCherry-positive cells), in P15 cortices targeted with Foxp2 or control (as in Fig. 5J,L), which also expressed Cux1 or Brn2 (Fig. 6E,F). We found that, upon ectopic expression of Foxp2, several of the targeted neurons that expressed Cux1 or Brn2 were

misplaced in deeper cortical layers or in the white matter (Fig. 6B-F). However, the proportion of targeted neurons that acquired an upper layer identity was unaffected (Fig. 6G,H). Taken together, these experiments indicate that differentiation of cortical projection neurons is not impaired after ectopic expression of Foxp2 protein.

Foxp2 has also been reported to be involved in the control of neurite outgrowth in neurons (Vernes et al., 2007; Spiteri et al., 2007; Reimers-Kipping et al., 2011; Vernes et al., 2011). Previous studies have shown that radial migration of cortical neurons requires precise coordination of leading process extension and branching (Nadarajah et al., 2001; Nadarajah et al., 2003; Kriegstein and Noctor, 2004; Attardo et al., 2008; Falnikar et al., 2011). Early stages of migration include polarization and processes extension (Dotti et al., 1988). To study whether ectopic expression of Foxp2 protein alters neurite outgrowth, we prepared primary neuronal cultures from embryonic cortices electroporated with pCAGGS empty plasmid, or pCAGGS-Foxp2-Δ-3′UTR, along with pCAGGS-mCherry plasmid (Fig. 6I-N). We then investigated neurite outgrowth specifically in cortical projection neurons (which were selectively targeted by mean of in utero electroporation of dTel) (LoTurco et al., 2009) by analyzing the total length (Fig. 6K,M) and branching (Fig. 6L,N) of neurites after 4 or 7 days in vitro (in wild-type animals, it is widely accepted that polarization and extension of neurites are already established within the first 4 days in vitro; Polleux and Snider, 2010). We found that, compared with controls, cortical projection neurons targeted with pCAGGS-Foxp2-Δ-*3′UTR* had shorter and less branched neurites at 4 days (Fig. 6I-L) but not at 7 days in vitro (Fig. 6M,N). This result indicates that ectopic expression of Foxp2 protein in developing cortical projection neurons alters the proper timing of neurite outgrowth. We speculate that this effect could explain the observed arrest in radial migration of neurons.

DISCUSSION

In our study, we used genome-wide profiling of miRNA-depleted embryonic mouse neocortex to identify potential miRNA target genes. We then validated in vivo one of the identified targets, *Foxp2*, and found that convergent action of miR-9 and miR-132 prevents ectopic expression of Foxp2 by targeting its 3′UTR. Moreover, we found that the ectopic expression of Foxp2 in developing projection neurons delays neurite outgrowth in vitro and impairs their radial migration in embryonic mouse neocortex in vivo.

Our study introduces a combined strategy of genome-wide profiling of miRNA-depleted embryonic mouse neocortex and in vivo target validation by in utero electroporation of Luciferase reporters, to experimentally validate novel miRNA targets with significance for neocortical development. Indeed, we have found more than 3000 genes that are regulated, either directly or indirectly, by the miRNA pathway in embryonic mouse neocortex. Which of these genes are directly controlled by miRNAs, and the function of such control in the orchestration of neocortical development are matters for continued study. Importantly, our in vivo validation of miRNA:mRNA interaction provides an improvement over the standard in vitro assays. Indeed, the cell-type specificity of miRNA regulation is increasingly recognized (Bhattacharyya et al., 2006; Jopling et al., 2005; Kedde et al., 2007; Vasudevan et al., 2007; Shibata et al., 2011).

The most remarkable finding of our study is that ectopic expression of Foxp2 in cortical projection neurons – a scenario that resembles the absence of miRNA-mediated repression of Foxp2 – delays neurite outgrowth and arrests their radial migration. This effect is attenuated by endogenous miR-9 and miR-132, which repress Foxp2 in embryonic neocortex. Foxp2 is involved in the fine control of neurite outgrowth in developing neurons (Enard et al., 2009; Reimers-Kipping et al., 2011; Tam et al., 2011; Vernes et al., 2011). Moreover, miR-9 and miR-132 are also involved in the control of neurite outgrowth and branching in neurons by targeting distinct subsets of mRNAs (Vo et al., 2005; Wayman et al., 2008; Xu et al., 2008). Our results therefore raise the intriguing possibility that, in migrating neurons, the precise coordination of neurite extension and branching is achieved by the convergent action of miR-9 and miR-132 to optimize *Foxp2* dose. Interestingly, miR-9 was recently found to tune levels of *Foxp1* (a paralog of *Foxp2*) to ensure proper development of motoneurons in developing chick spinal cord (Otaegi et al., 2011). Thus, miRNA-dependent repression of *Foxp* expression might be a broader mechanism that occurs in other members of the *Foxp* family.

Finally, numerous studies on the role of Foxp2 in neocortical development have focused on loss-of-function mutations (Shu et al., 2005; Groszer et al., 2008; Fujita et al., 2008; Takahashi et al., 2009). We found that ectopic expression of Foxp2 impairs neurite extension and radial migration of cortical projection neurons. Although we do not directly address the role of miR-9/132 in the control of endogenous Foxp2 expression [see Åkerblom et al. (Åkerblom et al., 2012) for extensive review about the current technical limitations in functional studies on miRNAs in vivo], we have uncovered a new layer of control of Foxp2 expression. Given that Foxp2 3′UTR and miR-9/132 are evolutionarily conserved, our finding sets the stage for future studies aimed at the direct investigation of mutations in the 3′UTR of human *FOXP2* transcript. These studies could perhaps provide new explanations for defects observed in human pathologies involving altered expression of FOXP genes (Hannenhalli and Kaestner, 2009).

Acknowledgements

We thank Dr L. Cancedda and Dr J. Assad (Istituto Italiano di Tecnologia, IIT) for critical reading of the manuscript; Dr Itohara (RIKEN, Japan) and Dr Hannon (Cold Spring Harbor Laboratory, MA, USA) for kindly providing *Emx1*^{Cre} and *Dicer*^{Flox} mouse lines, respectively; IIT and Max-Plank Institute of Molecular Cell Biology and Genetics (MPI-CBG) technical staff (M. Pesce, F. Succol, M. Nanni, F. Piccardi and C. Haffner) for help; B. Nickel and T. Giger [Max-Plank Institute of Evolutionary Anthropology (MPI-EVA)] for help in microarray experiments; and Dr Schwamborn (Münster University, Germany) for advice in miRNA inhibitors.

Funding

W.E. was supported by the Max-Planck Society; W.B.H. was supported by grants from the Deutsche Forschungsgemeinschaft (DFG) [SFB 655, A2; TRR 83, Tp6] and the ERC [250197], by the DFG-funded Center for Regenerative Therapies Dresden, and by the Fonds der Chemischen Industrie. This work was supported by Fondazione Istituto Italiano di Tecnologia.

Competing interests statement

The authors declare no competing financial interests.

Supplementary material

Supplementary material available online at
http://dev.biologists.org/lookup/suppl/doi:10.1242/dev.078063/-/DC1

References

Åkerblom, M., Sachdeva, R. and Jakobsson, J. (2012). Functional studies of microRNAs in neural stem cells: problems and perspectives. *Front. Neurosci.* **6**, 14.

Arvanitis, D. N., Jungas, T., Behar, A. and Davy, A. (2010). Ephrin-B1 reverse signaling controls a posttranscriptional feedback mechanism via miR-124. *Mol. Cell. Biol.* **30**, 2508-2517.

Ashburner, M., Ball, C. A., Blake, J. A., Botstein, D., Butler, H., Cherry, J. M., Davis, A. P., Dolinski, K., Dwight, S. S., Eppig, J. T. et al. (2000). Gene

ontology: tool for the unification of biology. The Gene Ontology Consortium. *Nat. Genet.* **25**, 25-29.
Attardo, A., Calegari, F., Haubensak, W., Wilsch-Bräuninger, M. and Huttner, W. B. (2008). Live imaging at the onset of cortical neurogenesis reveals differential appearance of the neuronal phenotype in apical versus basal progenitor progeny. *PLoS ONE* **3**, e2388.
Ayala, R., Shu, T. and Tsai, L. H. (2007). Trekking across the brain: the journey of neuronal migration. *Cell* **128**, 29-43.
Baek, D., Villén, J., Shin, C., Camargo, F. D., Gygi, S. P. and Bartel, D. P. (2008). The impact of microRNAs on protein output. *Nature* **455**, 64-71.
Betel, D., Koppal, A., Agius, P., Sander, C. and Leslie, C. (2010). Comprehensive modeling of microRNA targets predicts functional non-conserved and non-canonical sites. *Genome Biol.* **11**, R90.
Bhattacharyya, S. N., Habermacher, R., Martine, U., Closs, E. I. and Filipowicz, W. (2006). Relief of microRNA-mediated translational repression in human cells subjected to stress. *Cell* **125**, 1111-1124.
Brennecke, J., Stark, A., Russell, R. B. and Cohen, S. M. (2005). Principles of microRNA-target recognition. *PLoS Biol.* **3**, e85.
Campbell, P., Reep, R. L., Stoll, M. L., Ophir, A. G. and Phelps, S. M. (2009). Conservation and diversity of Foxp2 expression in muroid rodents: functional implications. *J. Comp. Neurol.* **512**, 84-100.
Candiani, S., Moronti, L., De Pietri Tonelli, D., Garbarino, G. and Pestarino, M. (2011). A study of neural-related microRNAs in the developing amphioxus. *Evodevo* **2**, 15.
Chekulaeva, M. and Filipowicz, W. (2009). Mechanisms of miRNA-mediated post-transcriptional regulation in animal cells. *Curr. Opin. Cell Biol.* **21**, 452-460.
Choi, P. S., Zakhary, L., Choi, W. Y., Caron, S., Alvarez-Saavedra, E., Miska, E. A., McManus, M., Harfe, B., Giraldez, A. J., Horvitz, H. R. et al. (2008). Members of the miRNA-200 family regulate olfactory neurogenesis. *Neuron* **57**, 41-55.
De Pietri Tonelli, D., Calegari, F., Fei, J. F., Nomura, T., Osumi, N., Heisenberg, C. P. and Huttner, W. B. (2006). Single-cell detection of microRNAs in developing vertebrate embryos after acute administration of a dual-fluorescence reporter/sensor plasmid. *Biotechniques* **41**, 727-732.
De Pietri Tonelli, D., Pulvers, J. N., Haffner, C., Murchison, E. P., Hannon, G. J. and Huttner, W. B. (2008). miRNAs are essential for survival and differentiation of newborn neurons but not for expansion of neural progenitors during early neurogenesis in the mouse embryonic neocortex. *Development* **135**, 3911-3921.
Dotti, C. G., Sullivan, C. A. and Banker, G. A. (1988). The establishment of polarity by hippocampal neurons in culture. *J. Neurosci.* **8**, 1454-1468.
Enard, W. (2011). FOXP2 and the role of cortico-basal ganglia circuits in speech and language evolution. *Curr. Opin. Neurobiol.* **21**, 415-424.
Enard, W., Przeworski, M., Fisher, S. E., Lai, C. S., Wiebe, V., Kitano, T., Monaco, A. P. and Pääbo, S. (2002). Molecular evolution of FOXP2, a gene involved in speech and language. *Nature* **418**, 869-872.
Enard, W., Gehre, S., Hammerschmidt, K., Hölter, S. M., Blass, T., Somel, M., Brückner, M. K., Schreiweis, C., Winter, C., Sohr, R. et al. (2009). A humanized version of Foxp2 affects cortico-basal ganglia circuits in mice. *Cell* **137**, 961-971.
Englund, C., Fink, A., Lau, C., Pham, D., Daza, R. A., Bulfone, A., Kowalczyk, T. and Hevner, R. F. (2005). Pax6, Tbr2, and Tbr1 are expressed sequentially by radial glia, intermediate progenitor cells, and postmitotic neurons in developing neocortex. *J. Neurosci.* **25**, 247-251.
Falnikar, A., Tole, S. and Baas, P. W. (2011). Kinesin-5, a mitotic microtubule-associated motor protein, modulates neuronal migration. *Mol. Biol. Cell* **22**, 1561-1574.
Ferland, R. J., Cherry, T. J., Preware, P. O., Morrisey, E. E. and Walsh, C. A. (2003). Characterization of Foxp2 and Foxp1 mRNA and protein in the developing and mature brain. *J. Comp. Neurol.* **460**, 266-279.
Fietz, S. A. and Huttner, W. B. (2011). Cortical progenitor expansion, self-renewal and neurogenesis – a polarized perspective. *Curr. Opin. Neurobiol.* **21**, 23-35.
Fisher, S. E. and Scharff, C. (2009). FOXP2 as a molecular window into speech and language. *Trends Genet.* **25**, 166-177.
Friedman, R. C., Farh, K. K., Burge, C. B. and Bartel, D. P. (2009). Most mammalian mRNAs are conserved targets of microRNAs. *Genome Res.* **19**, 92-105.
Fujita, E., Tanabe, Y., Shiota, A., Ueda, M., Suwa, K., Momoi, M. Y. and Momoi, T. (2008). Ultrasonic vocalization impairment of Foxp2 (R552H) knockin mice related to speech-language disorder and abnormality of Purkinje cells. *Proc. Natl. Acad. Sci. USA* **105**, 3117-3122.
Griffiths-Jones, S., Saini, H. K., van Dongen, S. and Enright, A. J. (2008). miRBase: tools for microRNA genomics. *Nucleic Acids Res.* **36**, D154-D158.
Groszer, M., Keays, D. A., Deacon, R. M., de Bono, J. P., Prasad-Mulcare, S., Gaub, S., Baum, M. G., French, C. A., Nicod, J., Coventry, J. A. et al. (2008). Impaired synaptic plasticity and motor learning in mice with a point mutation implicated in human speech deficits. *Curr. Biol.* **18**, 354-362.
Guo, H., Ingolia, N. T., Weissman, J. S. and Bartel, D. P. (2010). Mammalian microRNAs predominantly act to decrease target mRNA levels. *Nature* **466**, 835-840.
Hannenhalli, S. and Kaestner, K. H. (2009). The evolution of Fox genes and their role in development and disease. *Nat. Rev. Genet.* **10**, 233-240.
Hansen, K. F., Sakamoto, K., Wayman, G. A., Impey, S. and Obrietan, K. (2010). Transgenic miR132 alters neuronal spine density and impairs novel object recognition memory. *PLoS ONE* **5**, e15497.
Hendrickson, D. G., Hogan, D. J., McCullough, H. L., Myers, J. W., Herschlag, D., Ferrell, J. E. and Brown, P. O. (2009). Concordant regulation of translation and mRNA abundance for hundreds of targets of a human microRNA. *PLoS Biol.* **7**, e1000238.
Hisaoka, T., Nakamura, Y., Senba, E. and Morikawa, Y. (2010). The forkhead transcription factors, Foxp1 and Foxp2, identify different subpopulations of projection neurons in the mouse cerebral cortex. *Neuroscience* **166**, 551-563.
Iwasato, T., Datwani, A., Wolf, A. M., Nishiyama, H., Taguchi, Y., Tonegawa, S., Knöpfel, T., Erzurumlu, R. S. and Itohara, S. (2000). Cortex-restricted disruption of NMDAR1 impairs neuronal patterns in the barrel cortex. *Nature* **406**, 726-731.
Jopling, C. L., Yi, M., Lancaster, A. M., Lemon, S. M. and Sarnow, P. (2005). Modulation of hepatitis C virus RNA abundance by a liver-specific microRNA. *Science* **309**, 1577-1581.
Kawase-Koga, Y., Otaegi, G. and Sun, T. (2009). Different timings of Dicer deletion affect neurogenesis and gliogenesis in the developing mouse central nervous system. *Dev. Dyn.* **238**, 2800-2812.
Kedde, M., Strasser, M. J., Boldajipour, B., Oude Vrielink, J. A., Slanchev, K., le Sage, C., Nagel, R., Voorhoeve, P. M., van Duijse, J., Ørom, U. A. et al. (2007). RNA-binding protein Dnd1 inhibits microRNA access to target mRNA. *Cell* **131**, 1273-1286.
Kriegstein, A. R. and Noctor, S. C. (2004). Patterns of neuronal migration in the embryonic cortex. *Trends Neurosci.* **27**, 392-399.
Krol, J., Loedige, I. and Filipowicz, W. (2010). The widespread regulation of microRNA biogenesis, function and decay. *Nat. Rev. Genet.* **11**, 597-610.
Lagos-Quintana, M., Rauhut, R., Yalcin, A., Meyer, J., Lendeckel, W. and Tuschl, T. (2002). Identification of tissue-specific microRNAs from mouse. *Curr. Biol.* **12**, 735-739.
Lai, C. S., Fisher, S. E., Hurst, J. A., Vargha-Khadem, F. and Monaco, A. P. (2001). A forkhead-domain gene is mutated in a severe speech and language disorder. *Nature* **413**, 519-523.
Lai, C. S., Gerrelli, D., Monaco, A. P., Fisher, S. E. and Copp, A. J. (2003). FOXP2 expression during brain development coincides with adult sites of pathology in a severe speech and language disorder. *Brain* **126**, 2455-2462.
Lai, E. C. (2002). Micro RNAs are complementary to 3′ UTR sequence motifs that mediate negative post-transcriptional regulation. *Nat. Genet.* **30**, 363-364.
Lambert, T. J., Storm, D. R. and Sullivan, J. M. (2010). MicroRNA132 modulates short-term synaptic plasticity but not basal release probability in hippocampal neurons. *PLoS ONE* **5**, e15182.
Langevin, L. M., Mattar, P., Scardigli, R., Roussigné, M., Logan, C., Blader, P. and Schuurmans, C. (2007). Validating in utero electroporation for the rapid analysis of gene regulatory elements in the murine telencephalon. *Dev. Dyn.* **236**, 1273-1286.
Lewis, B. P., Burge, C. B. and Bartel, D. P. (2005). Conserved seed pairing, often flanked by adenosines, indicates that thousands of human genes are microRNA targets. *Cell* **120**, 15-20.
Li, S., Weidenfeld, J. and Morrisey, E. E. (2004). Transcriptional and DNA binding activity of the Foxp1/2/4 family is modulated by heterotypic and homotypic protein interactions. *Mol. Cell. Biol.* **24**, 809-822.
LoTurco, J., Manent, J. B. and Sidiqi, F. (2009). New and improved tools for in utero electroporation studies of developing cerebral cortex. *Cereb. Cortex* **19 Suppl. 1**, i120-i125.
Lui, J. H., Hansen, D. V., and Kriegstein A. R. (2011). Development and evolution of the human neocortex. *Cell* **146**, 18-36.
Magill, S. T., Cambronne, X. A., Luikart, B. W., Lioy, D. T., Leighton, B. H., Westbrook, G. L., Mandel, G. and Goodman, R. H. (2010). microRNA-132 regulates dendritic growth and arborization of newborn neurons in the adult hippocampus. *Proc. Natl. Acad. Sci. USA* **107**, 20382-20387.
Makeyev, E. V., Zhang, J., Carrasco, M. A. and Maniatis, T. (2007). The MicroRNA miR-124 promotes neuronal differentiation by triggering brain-specific alternative pre-mRNA splicing. *Mol. Cell* **27**, 435-448.
Meijering, E., Jacob, M., Sarria, J.-C. F., Steiner, P., Hirling, H. and Unser, M. (2004). Design and validation of a tool for neurite tracing and analysis in fluorescence microscopy images. *Cytometry* **58**, 167-176.
Molyneaux, B. J., Arlotta, P., Menezes, J. R. and Macklis, J. D. (2007). Neuronal subtype specification in the cerebral cortex. *Nat. Rev. Neurosci.* **8**, 427-437.
Murchison, E. P., Partridge, J. F., Tam, O. H., Cheloufi, S. and Hannon, G. J. (2005). Characterization of Dicer-deficient murine embryonic stem cells. *Proc. Natl. Acad. Sci. USA* **102**, 12135-12140.

Muzio, L., Di Benedetto, B., Stoykova, A., Boncinelli, E., Gruss, P. and Mallamaci, A. (2002). Emx2 and Pax6 control regionalization of the pre-neuronogenic cortical primordium. *Cereb. Cortex* **12**, 129-139.
Nadarajah, B., Brunstrom, J. E., Grutzendler, J., Wong, R. O. and Pearlman, A. L. (2001). Two modes of radial migration in early development of the cerebral cortex. *Nat. Neurosci.* **4**, 143-150.
Nadarajah, B., Alifragis, P., Wong, R. O. and Parnavelas, J. G. (2003). Neuronal migration in the developing cerebral cortex: observations based on real-time imaging. *Cereb. Cortex* **13**, 607-611.
Nakagawa, Y., Johnson, J. E. and O'Leary, D. D. (1999). Graded and areal expression patterns of regulatory genes and cadherins in embryonic neocortex independent of thalamocortical input. *J. Neurosci.* **19**, 10877-10885.
Niwa, H., Yamamura, K. and Miyazaki, J. (1991). Efficient selection for high-expression transfectants with a novel eukaryotic vector. *Gene* **108**, 193-199.
Olde Loohuis, N. F., Kos, A., Martens, G. J., Van Bokhoven, H., Nadif Kasri, N. and Aschrafi, A. (2012). MicroRNA networks direct neuronal development and plasticity. *Cell. Mol. Life Sci.* **69**, 89-102.
Otaegi, G., Pollock, A., Hong, J. and Sun, T. (2011). MicroRNA miR-9 modifies motor neuron columns by a tuning regulation of FoxP1 levels in developing spinal cords. *J. Neurosci.* **31**, 809-818.
Pinto, L. and Götz, M. (2007). Radial glial cell heterogeneity–the source of diverse progeny in the CNS. *Prog. Neurobiol.* **83**, 2-23.
Polleux, F. and Snider, W. (2010). Initiating and growing an axon. *Cold Spring Harb. Perspect. Biol.* **2**, a001925.
Prüfer, K., Muetzel, B., Do, H. H., Weiss, G., Khaitovich, P., Rahm, E., Pääbo, S., Lachmann, M. and Enard, W. (2007). FUNC: a package for detecting significant associations between gene sets and ontological annotations. *BMC Bioinformatics* **8**, 41.
Reimers-Kipping, S., Hevers, W., Pääbo, S. and Enard, W. (2011). Humanized Foxp2 specifically affects cortico-basal ganglia circuits. *Neuroscience* **175**, 75-84.
Saba, R. and Schratt, G. M. (2010). MicroRNAs in neuronal development, function and dysfunction. *Brain Res.* **1338**, 3-13.
Saito, T. and Nakatsuji, N. (2001). Efficient gene transfer into the embryonic mouse brain using in vivo electroporation. *Dev. Biol.* **240**, 237-246.
Selbach, M., Schwanhäusser, B., Thierfelder, N., Fang, Z., Khanin, R. and Rajewsky, N. (2008). Widespread changes in protein synthesis induced by microRNAs. *Nature* **455**, 58-63.
Shibata, M., Kurokawa, D., Nakao, H., Ohmura, T. and Aizawa, S. (2008). MicroRNA-9 modulates Cajal-Retzius cell differentiation by suppressing Foxg1 expression in mouse medial pallium. *J. Neurosci.* **28**, 10415-10421.
Shibata, M., Nakao, H., Kiyonari, H., Abe, T. and Aizawa, S. (2011). MicroRNA-9 regulates neurogenesis in mouse telencephalon by targeting multiple transcription factors. *J. Neurosci.* **31**, 3407-3422.
Shu, W., Yang, H., Zhang, L., Lu, M. M. and Morrisey, E. E. (2001). Characterization of a new subfamily of winged-helix/forkhead (Fox) genes that are expressed in the lung and act as transcriptional repressors. *J. Biol. Chem.* **276**, 27488-27497.
Shu, W., Cho, J. Y., Jiang, Y., Zhang, M., Weisz, D., Elder, G. A., Schmeidler, J., De Gasperi, R., Sosa, M. A., Rabidou, D. et al. (2005). Altered ultrasonic vocalization in mice with a disruption in the Foxp2 gene. *Proc. Natl. Acad. Sci. USA* **102**, 9643-9648.
Simeone, A., Gulisano, M., Acampora, D., Stornaiuolo, A., Rambaldi, M. and Boncinelli, E. (1992). Two vertebrate homeobox genes related to the Drosophila empty spiracles gene are expressed in the embryonic cerebral cortex. *EMBO J.* **11**, 2541-2550.
Spiteri, E., Konopka, G., Coppola, G., Bomar, J., Oldham, M., Ou, J., Vernes, S. C., Fisher, S. E., Ren, B. and Geschwind, D. H. (2007). Identification of the transcriptional targets of FOXP2, a gene linked to speech and language, in developing human brain. *Am. J. Hum. Genet.* **81**, 1144-1157.
Takahashi, K., Liu, F. C., Hirokawa, K. and Takahashi, H. (2003). Expression of Foxp2, a gene involved in speech and language, in the developing and adult striatum. *J. Neurosci. Res.* **73**, 61-72.
Takahashi, K., Liu, F. C., Hirokawa, K. and Takahashi, H. (2008). Expression of Foxp4 in the developing and adult rat forebrain. *J. Neurosci. Res.* **86**, 3106-3116.
Takahashi, H., Takahashi, K. and Liu, F. C. (2009). FOXP genes, neural development, speech and language disorders. *Adv. Exp. Med. Biol.* **665**, 117-129.
Tam, W. Y., Leung, C. K., Tong, K. K. and Kwan, K. M. (2011). Foxp4 is essential in maintenance of Purkinje cell dendritic arborization in the mouse cerebellum. *Neuroscience* **172**, 562-571.
Thomas, M., Lieberman, J. and Lal, A. (2010). Desperately seeking microRNA targets. *Nat. Struct. Mol. Biol.* **17**, 1169-1174.
Vasudevan, S., Tong, Y. and Steitz, J. A. (2007). Switching from repression to activation: microRNAs can up-regulate translation. *Science* **318**, 1931-1934.
Vernes, S. C., Spiteri, E., Nicod, J., Groszer, M., Taylor, J. M., Davies, K. E., Geschwind, D. H. and Fisher, S. E. (2007). High-throughput analysis of promoter occupancy reveals direct neural targets of FOXP2, a gene mutated in speech and language disorders. *Am. J. Hum. Genet.* **81**, 1232-1250.
Vernes, S. C., Oliver, P. L., Spiteri, E., Lockstone, H. E., Puliyadi, R., Taylor, J. M., Ho, J., Mombereau, C., Brewer, A., Lowy, E. et al. (2011). Foxp2 regulates gene networks implicated in neurite outgrowth in the developing brain. *PLoS Genet.* **7**, e1002145.
Vo, N., Klein, M. E., Varlamova, O., Keller, D. M., Yamamoto, T., Goodman, R. H. and Impey, S. (2005). A cAMP-response element binding protein-induced microRNA regulates neuronal morphogenesis. *Proc. Natl. Acad. Sci. USA* **102**, 16426-16431.
Wayman, G. A., Davare, M., Ando, H., Fortin, D., Varlamova, O., Cheng, H. Y., Marks, D., Obrietan, K., Soderling, T. R., Goodman, R. H. et al. (2008). An activity-regulated microRNA controls dendritic plasticity by down-regulating p250GAP. *Proc. Natl. Acad. Sci. USA* **105**, 9093-9098.
Xu, X. L., Li, Y., Wang, F. and Gao, F. B. (2008). The steady-state level of the nervous-system-specific microRNA-124a is regulated by dFMR1 in Drosophila. *J. Neurosci.* **28**, 11883-11889.
Yuva-Aydemir, Y., Simkin, A., Gascon, E. and Gao, F. B. (2011). MicroRNA-9: functional evolution of a conserved small regulatory RNA. *RNA Biol.* **8**, 557-564.
Zhao, C., Sun, G., Li, S. and Shi, Y. (2009). A feedback regulatory loop involving microRNA-9 and nuclear receptor TLX in neural stem cell fate determination. *Nat. Struct. Mol. Biol.* **16**, 365-371.
Zhao, C., Sun, G., Li, S., Lang, M. F., Yang, S., Li, W. and Shi, Y. (2010). MicroRNA let-7b regulates neural stem cell proliferation and differentiation by targeting nuclear receptor TLX signaling. *Proc. Natl. Acad. Sci. USA* **107**, 1876-1881.